Nitric oxide and cyclic GMP increase the expression of matrix metalloproteinase-9 in vascular smooth muscle.

Authors: Marcelo Marcet-Palacios [1,5], Kathryn Graham [2,4], Carol Cass [2,4], A. Dean Befus [1,5], Irvin Mayers [1], Marek W. Radomski [3].

Department of Medicine, University of Alberta, Edmonton, Alberta, Canada (1).

JPET #050385

Running title: Nitric oxide and cGMP increase the expression of MMP-9.

Corresponding author: Dr. A. Dean Befus, Chair in Asthma Research, AstraZeneca Canada Inc., Glaxo-Heritage Asthma Research Laboratories, Department of Medicine, University of Alberta, Edmonton, AB, T6G 2S2, Canada. Tel: 1 (780) 492 1909, Fax: 1 (780) 492 5329. E-mail: dean.befus@ualberta.ca

Text pages 24

Tables 2

Figures 7

References 39

Words in Abstract 222

Words in Introduction 449

Words in Discussion 1190

Non-standard abbreviations: ODQ, 1H-[1,2,4] oxadiazolo [4,3-a] quinoxalin-1-one; IFN-γ, interferon gamma; SOD, superoxide dismutase; LPS, bacterial lipopolysaccharide; PMA, phorbol 12-myristate13-acetate; GAPDH, glyceraldehyde-3-phosphate dehydrogenase; Dex, dexamethasone; cGMP, cyclic guanosine monophosphate; BLAST, basic local alignment search tool; PGE_2, prostaglandin E2; O_2^-, superoxide; $ONOO^-$, peroxynitrite; MnTMPyP, Mn(III)tetrakis(1-methyl-4-pyridyl)porphyrin pentachloride and 8-bromo-cGMP, guanosine 3',5'-cyclic monophosphate 8-bromo.

Section assignment: Cellular & Molecular.

JPET #050385

Abstract:

Interactions and possible cross-talk between inducible nitric oxide synthase (iNOS), cyclooxygenase-2 (COX-2) and matrix metalloproteinase-9 (MMP-9), were studied in rat aortic vascular smooth muscle cells stimulated with bacterial lipopolysaccharide (LPS), interferon-γ (IFN-γ) and phorbol 12-myristate13-acetate (PMA). The expression and activity of iNOS, COX-2 and MMP-9 were characterized at the transcriptional, protein and the enzyme activity levels. The NOS inhibitor L-nitro-arginine methyl ester (L-NAME) was used to investigate the effects of NO on COX-2 and MMP-9 at the transcriptional level. The measurements of mRNAs for these enzymes using real time PCR showed that COX-2 mRNA was upregulated 2.3 fold, whereas MMP-9 mRNA upregulation was 11.7 fold, in the presence of LPS, IFN-γ and PMA. Real time PCR results indicated that L-NAME exerted an inhibitory effect on COX-2 and MMP-9 mRNA synthesis. Both superoxide dismutase and the SOD mimetic Mn(III)tetrakis(1-Methyl-4-pyridyl)porphyrin Pentachloride (MnTMPyP) did not modify significantly the upregulation of these enzymes, indicating that neither superoxide nor peroxynitrite are involved in this mechanism. Furthermore, NO-mediated upregulation of MMP-9 was cyclic guanosine monophosphate (cGMP)-dependent since 1H-[1,2,4] Oxadiazolo [4,3-a] quinoxalin-1-one (ODQ), an inhibitor of soluble guanylate cyclase, blocked, in a concentration dependent manner, the increased expression of MMP-9, an effect reversed by guanosine 3',5'-cyclic monophosphate 8-bromo (8-bromo-cGMP), a soluble analog of cGMP. Our findings suggest that NO and cGMP are necessary to upregulate the expression of MMP-9.

Septic shock is characterized by severe hypotension, hyporesponsiveness to vasoconstrictors and volume depletion leading to multiorgan dysfunction and death (Bone, 1994; Webber, 1998). This condition is a complex endotoxin-induced systemic inflammatory response, which affects more than 400,000 patients per year in the United States (Knuefermann et al., 2002). Cell wall-endotoxins such as bacterial lipopolysaccharide (LPS) are largely responsible for the pathogenesis of this disease. The endothelium and the vascular smooth muscle are among major cellular targets of LPS (Alexander and Rietschel, 2001).

The deleterious effects of LPS are often mediated by the enzymatic activity of LPS-inducible proteins such as inducible nitric oxide synthase (iNOS), cyclooxygenase-2 (COX-2) and matrix metalloproteinase-9 (MMP-9). Initially, these enzymes are induced in a highly organized fashion to compensate for the damaging effects of LPS and maintain homeostasis, and to contribute to the systemic inflammatory response. However, the overwhelming concentrations of these inducible enzymes can become harmful to the body, contributing to multiorgan dysfunction and death. The increased expression of iNOS, for example, results in massive vasodilatation and hypotension (Gomez-Jimenez et al., 1995; Titheradge, 1999). Additionally, fast reaction of NO with superoxide (O_2^-) leads to the highly reactive species, peroxynitrite ($ONOO^-$) (Beckman et al., 1990; Beckman and Koppenol, 1996). The latter, is thought to be responsible for many deleterious effects of NO, acting as an oxidant itself or leading to the formation of other reactive species (Szabo et al., 1996). Moreover, COX-2 upregulation leads to overproduction of thromboxane and prostaglandin E_2 (PGE_2), which have been implicated in the pathogenesis of septic shock (Ermert et al., 2000; Fischer et al., 2000; Strong et al., 2000). In the presence of LPS, cells like neutrophils secrete considerable amounts of latent MMPs, including MMP-9 (Albert et al., 2003). Reactive oxygen species, produced by the same cell type, lead to the chemical activation of MMP-9 and as a consequence, degradation of the vascular wall takes place (Opdenakker, 2001). Other lines of evidence from mice and humans have also correlated MMP-9 levels with shock conditions (Pugin et al., 1999; Dubois et al., 2002; Albert et al., 2003).

Despite solid evidence that iNOS, COX-2 and MMP-9 are involved in the pathogenesis of cellular damage caused by LPS, the interactions (cross-talk) between these enzymes are unclear. We found that the simultaneous induction of these enzymes could be triggered by IFN-γ, PMA and LPS in rat vascular smooth muscle (VSM) cells, allowing us to study the hypothesis that these three enzymes cross-talk to each other.

4

The production of these three enzymes was studied at the transcriptional level, at the protein level and at the

enzyme activity level. The results of our experiments provide evidence that iNOS upregulates COX-2 and

MMP-9 gene expression in VSM.

Materials and Methods:

Materials: Polyclonal antibodies against iNOS and COX-2 were obtained from BD Transduction Laboratories (Basingtoke, Hampshire, UK) and Santa Cruz Biotechnology Inc (Santa Cruz, California, U.S.A.) respectively. Monoclonal antibodies against MMP-9 were obtained from Oncogene Research Products (Cambridge, MA, U.S.A). RNeasy Mini Kit was obtained from Qiagene Inc (Mississauga, Ontario, Canada).

Cell culture: Rat aortic VSM (A7r5) were obtained from American Type Culture Collection. Cells were cultured in $75cm^2$ flasks in a humidified atmosphere with 5% CO_2 at 37^oC. The medium was Dulbecco's modified eagle's medium (DMEM) supplemented to contain 4.5g/L glucose and 1.5 g/L sodium bicarbonate, 10% fetal bovine serum (FBS) and gentamycin sulfate (0.05 mg/mL), penicillin G (0.06 mg/mL) and streptomycin sulfate (0.01 mg/mL). Cells were grown until they were confluent and then treated for 12 h with a cocktail containing 10 ng/mL IFN-γ, 1nM PMA, 10μg/mL LPS in 15mL of 1% FBS (activating cocktail). When treating with dexamethasone (Dex), cells were pre-incubated with this chemical for 1 h prior to induction with the activating cocktail. Dex concentrations of 1.0, 3.0 and 10 μM were tested. At a concentration of 1μM, Dex did not confer inhibitory effects as detectable by RT-PCR. 3μM Dex was found to be sufficient to inhibit transcription of iNOS, COX-2 and MMP-9 and all consecutive experiments were performed using 3 μM Dex. When either L-NAME (300μM); ODQ (0.05, 0.1, 0.5, 1.0, and 5 μM); or superoxide dismutase (SOD) (0.5, 1, 5, 10, 100 U/mL) where used, these compounds were included in the activating cocktail. Cell harvesting was conducted by scraping cells off plates in the presence of 1mL homogenizing buffer (50 mM Tris-HCl, 320 mM sucrose, 1 mM dithiothreitol, 10 μg/mL leupeptin, 10 μg/mL soybean trypsin inhibitor, 2 μg/mL aprotinin, pH 7.4).

Gelatin Zymography: This technique was used to measure pro and active MMP-2 and MMP-9 gelatinolytic activity as previously described (Radomski et al., 1998). After cell extraction, samples were immediately subjected to electrophoresis on 7% SDS-PAGE co-polymerized with gelatin (2mg/mL) as the substrate. Independent experiments were performed and run on the same gel. Following electrophoresis, gels were washed in Triton X-100 (0.1%; 3 times, 20 min). The gels were then incubated for 72 h in the zymography buffer containing 25mM Tris/Cl, 5mM $CaCl_2$, 142mM NaCl and 0.5mM Na_3N to determine the activity of secreted enzymes. After incubation, the gels were stained with 0.05% Coomassie brilliant blue G-250 in a mixture of methanol: acetic acid: water (2.5: 1: 6.5) and destained in 4% methanol with 8% acetic acid. The

6

gelatinolytic activities were detected as transparent bands against the background of Coomassie blue-stained gelatin. Enzyme activity was assayed by densitometry using a ScanJet 3c scanner and SigmaGel measurement software. The pro and active forms of MMP-9 were identified as bands at 92 and 88 kDa respectively.

Inducible and constitutive nitric oxide synthase activity assay (citrulline assay): Nitric oxide synthase activity in A7r5 cell homogenate was assessed by measuring the formation of L-[^{14}C]-citrulline from L-[U-^{14}C]-arginine as previously described (Radomski et al., 1993). Briefly, samples were homogenized by sonication (VibraCell, Danbury, CT) in 1 mL of ice-cold homogenizing buffer followed by centrifugation at 10,000 x g for 20 min at 4 ºC. Following centrifugation, 40 µl of supernatant was incubated at 37ºC for 20 min in assay buffer (pH 7.4) containing 50 mM KH_2PO_4, 1 mM $MgCl_2$, 0.2 mM $CaCl_2$, 1 mM L-citrulline, 20 µM L-arginine, 1.5 mM dithiothreitol, 1.5 mM NADPH, 10 µM tetrahydrobiopterin, 10 µM FAD, 10 µM FMN and 0.5 µCi/mL U-^{14}C-L-arginine. The specificity of L-arginine conversion by NOS to L-citrulline was further confirmed using 1.2 mM N^{ω}-nitro-L-arginine methyl ester, a selective inhibitor of NOS. Additionally, 1.5 mM EGTA, a calcium chelating agent, was used to differentiate between Ca^{2+}-dependent and -independent isoforms of NOS. All enzyme activities were expressed as pmol product generated per min per mg protein. The limit of detection of this method was 0.05 pmol/min/mg protein.

Griess assay: Formation of NO_2^- was measured as previously described (Gilchrist et al., 2002). Briefly, 50µl of supernatant was measured by the Griess reaction. Results were expressed as µM/10^6 cells following incubation for 6, 12, 24, 48 and 72h. Equal volumes of cell-free supernatant and Griess reagent (1% sulfanilamine, 0.1% N-(1-naphyl)-ethylene-diamine dihydrochloride, 2.5% H_3PO_4) were mixed. NaNO2 was used as a standard. Plates were read on a Vmax kinetic microplate reader (Molecular Devices Co., Menol Park, CA) at 540 nm.

Live-cell fluorescence determination of intracellular NO: NO production by A7r5 was assayed using DAF-FM, a cell-permeable NO-sensitive fluorescent dye as previously described (Grisham et al., 1999). Cells were incubated for 1h with 10µM DAF-FM, prior to visualization.

Cyclooxygenase-2 enzyme immuno assay: The activity of COX-2 was measured using a prostaglandin E_2 enzyme-immunoassay kit (Amersham Pharmacia Biotech, NJ, U.S.A.) according to manufacturer's instructions. The amounts of PGE_2 were expressed in pg/well of PGE_2 with each well containing a cell concentration of 10^5.

JPET #050385

Immuno-blot detection: The cells were harvested, homogenized in the homogenization buffer. The homogenates were subjected to 7% SDS-PAGE (Radomski et al., 1998) and proteins were identified using anti-MMP-9 antibodies (0.2µg/mL; Oncogen Science), anti-COX-2 antibodies (2µg/mL; Santa Cruz Biotechnology Inc) and anti-iNOS antibodies (0.125µg/mL; BD Transduction Laboratories).

RT-PCR and quantitative real time PCR: Experiments were performed as previously described (Szkotak et al., 2001). Total RNA was isolated using the Qiagen RNeasy kit. The RNA was reverse transcribed with the use of Superscript II reverse transcriptase (Gibco BRL) using oligo(dT) as primers. Thereafter, PCR was performed in 20µL reactions with the primer pairs (25 µM) described in Table 1. Glyceraldehyde-3-phosphate dehydrogenase (GAPDH)- specific primers were run in all reactions as the internal positive control. The PCR products were amplified for 30 cycles. The selected cycle number was chosen to stop the PCR reaction during its log phase to ensure availability of all reagents. Additional RT-PCR-related information is summarized in Table 1.

Quantitative Real Time PCR: Real time PCR experiments were performed using the TaqMan™ quantitative RT-PCR reaction (Applied Biosystems) as previously described (Ritzel et al., 2001). Briefly, an oligonucleotide probe, labeled with a fluorescent tag at the 5'-end and a quenching molecule at the 3'-end, is hybridized between two PCR primers at the beginning of the reaction. The 5'-nucleotidase activity of Taq polymerase, cleaves the fluorescent dye from the probe during each PCR cycle. The fluorescent signal generated is monitored in real time and is proportional to the amount of starting template in the sample. Real time PCR products were cloned and sequenced to confirm the identity of the mRNAs. The primer and probe sequences are summarized in Table 2.

Reagents: Other PCR related chemicals such as 100 bp DNA ladder, superscript II, Taq DNA polymerase, and oligo(dT) primer were obtained from Gibco BRL; whereas dNTP and RNaseOUT ribonuclease were obtained from Invitrogen. Phorbol 12-myristate13-acetate (PMA), ethidium bromide, interferon-gamma, lipopolysaccharide, dexamethasone crystalline, N^w-nitro-L-arginine methyl ester (L-NAME) (Alexis Corporation, San Diego, CA), N^G-monomethyl-L-arginine (L-NMMA), 1H-[1,2,4] oxadiazolo [4,3-a] quinoxalin-1-one (ODQ), and superoxide dismutase were obtained from Sigma (Oakville, Ontario, Canada). Mn(III)tetrakis(1-methyl-4-pyridyl)porphyrin mentachloride (MnTMPyP) and guanosine 3',5'-cyclic monophosphate 8-bromo (8-bromo-cGMP) were obtained from Calbiochem (Mississauga, Ontario Canada).

8

JPET #050385

U-^{14}C-L-arginine was obtained from Amersham, Oakville, ON and   AG50W-X8 resin was obtained from Bio-Rad.

Statistics: Results are means ± SE of at least three independent experiments. They were analyzed using one-way ANOVA and when significant differences were found the multiple-comparison Tukey-Kramer test was used (GraphPad InStat). Values where $P<0.05$ were considered statistically significant.

Results:

Since the objective of this research was to investigate the interactions between COX-2, iNOS and MMP-9 in VSM we have first tested various combinations of cytokine/inducing agents to cause simultaneous induction of these enzymes. The following combinations have been tested. A concentration gradient of 0.01, 0.1, 1 and 10μg/mL LPS did not produce a band detectable by zymography or RT-PCR for MMP-9, but constitutive MMP-2 activity was constant for every treatment (data not shown). 100nM PMA produced detectable bands for MMP-9 through RT-PCR and zymography, but did not activate iNOS mRNA as detectable by RT-PCR (data not shown). IFN-γ at a concentration of 1 mg/mL did not induce any of the mRNA signals for iNOS, COX-2 or MMP-9 (data not shown). After these preliminary experiments a combination containing 0.1ng/mL IFN-γ, 10 μg/mL LPS and 1nM PMA was found to be most effective in enzyme induction and all subsequent experiments were performed with cells stimulated with IFN-γ, LPS and PMA. Initial experiments were done using this cocktail and a time course for MMP-9 activity indicated optimal expression by 12h after activation (data not shown).

A time course of NO_2^- formation using the Griess reaction showed that there was a significant increase in nitrite formation after 24h (13.9±6.03μM) and after 48h (37.6±1.2μM) of cell activation. Nitrite formation was not detected in control conditions or when activated cells were co-treated with either L-NAME (300 μM) or 1400W (10nM) ($n = 3$). A more sensitive fluorimetric assay using the fluorochrome DAF showed NO production by 12h after cell induction (Fig. 1).

To study enzyme induction at the transcriptional level, Reverse Transcription-Polymerase Chain Reaction (RT-PCR) was used. Primers were developed and analyzed using the BLAST sequencing program at Grenbank to ensure unique complementation. When A7r5 cells were exposed to the activating cocktail, the mRNAs for iNOS, COX-2 and MMP-9 were markedly upregulated (Fig. 2-A and 2-B). The PCR products for all templates were identified at their predicted molecular weights of 241, 347, 664 and 528bp for MMP-9, iNOS, COX-2 and GAPDH, respectively (Fig. 2-A). The induction of iNOS, COX-2 and MMP-9 mRNAs was significantly inhibited by 3μM Dex (Fig. 2-B and 2-C). The housekeeping gene GAPDH was amplified for each experiment and used as the internal positive control. GAPDH mRNA levels were not significantly changed by different treatments (Fig. 2-B).

JPET #050385

To investigate if protein levels for these enzymes were affected by the treatment, western blot experiments were conducted using the same experimental conditions. We found that the levels of iNOS, COX-2 and MMP-9 proteins were increased by the treatment with the activating cocktail and this enhancement was abolished in the presence of dexamethasone (Fig. 3A-C).

The enzymatic activities of iNOS, COX-2 and MMP-9 were also characterized. The activity of Ca^{2+}-independent NOS in unstimulated (Sham) VSM was 12.4 ± 0.6 pmol/mg protein/min (Fig 4A). Cell induction resulted in a significant increase in the activity of this enzyme to 24.4 ± 2.6 pmol/mg protein/min. Ca^{2+}-dependent NOS activity was not detectable under these conditions, indicating that neither nNOS or eNOS were expressed in A7r5.

The activity of COX-2, as measured by prostaglandin E_2 (PGE_2) levels, was significantly increased following cell induction, (Fig. 4-B). The gelatinolytic activity of MMP-9, but not MMP-2, was markedly upregulated by the activating cocktail (Fig. 4-C). Dexamethasone abolished increases in iNOS, COX-2 and MMP-9 activities caused by cell induction (Fig. 4A-C).

Effects of L-NAME on COX-2 and MMP-9 transcription: Inhibition of NOS with L-NAME ($300\mu M$) exerted no significant effect on iNOS mRNA expression in activated cells (Fig. 5-A). In contrast, COX-2 and MMP-9 transcription was downregulated by this inhibitor (Fig. 5-A). L-NAME did not change the expression levels of the positive control GAPDH. To quantify the changes detected using RT-PCR, real time PCR analysis was conducted for COX-2 and MMP-9 mRNAs. It was found that COX-2 was upregulated by 2.3 fold (Fig. 5-C) and that this upregulation could be inhibited to lower than control levels by either Dex or L-NAME. MMP-9 mRNA levels were upregulated with the activating cocktail by approximately 11.7 times and they were significantly reduced in the presence of Dex or L-NAME (Fig. 5-B).

Effects of SOD and MnTMPyP on MMP-9 mRNA: To investigate if superoxide and possibly peroxynitrite (Patel et al., 1999) were involved in MMP-9 regulation by iNOS the scavenger of superoxide, superoxide dismutase (SOD), was tested on A7r5 cells induced with the activating cocktail. SOD at concentrations of 100, 10, 5, 1, and 0.5 U/mL exerted no significant effects on MMP-9 mRNA induction (Fig. 6-A). These concentrations of SOD effectively blocked superoxide generation by xanthine oxidase (Ohara et al., 1993) (data not shown). The membrane-soluble SOD mimetic MnTMPyP did not modify significantly the

11

upregulation of these enzymes indicating that neither superoxide nor peroxynitrite are involved in this mechanism (Fig. 6-B).

Effects of 1H-[1,2,4] Oxadiazolo [4,3-a] quinoxalin-1-one (ODQ) and 8-bromo-cGMP on MMP-9 mRNA regulation: To study the involvement of cyclic guanosine monophosphate (cGMP) in MMP-9 mRNA regulation ODQ, an inhibitor of soluble guanylate cyclase (sGC) was used. ODQ effectively decreased, in a concentration dependent fashion, the levels of MMP-9 mRNA (Fig. 7-A). 8-bromo-cGMP, a soluble analog of cGMP, reversed the effect of ODQ (Fig. 7-B).

JPET #050385

Discussion:

We have investigated the interactions between iNOS, COX-2 and MMP-9, three pro-inflammatory enzymes that are induced in the vasculature during acute inflammatory reactions such as septicemia and septic shock (Beckman et al., 1990; Gomez-Jimenez et al., 1995; Beckman and Koppenol, 1996; Szabo et al., 1996; Pugin et al., 1999; Titheradge, 1999; Ermert et al., 2000; Fischer et al., 2000; Strong et al., 2000; Opdenakker, 2001; Dubois et al., 2002; Albert et al., 2003). We have studied these interactions using rat smooth muscle vascular cells, which were induced by LPS, IFN-γ and PMA. Under experimental conditions used, the inducing agents resulted in upregulation of enzyme expression at transcriptional (mRNA), translational (protein) and activity (product generation or substrate degradation) levels. We have further validated our model of simultaneous induction of iNOS, COX-2 and MMP-9 using dexamethasone, a potent glucocorticoid known to inhibit many pathways of inflammation . As expected this drug treatment efficiently reduced the expression of iNOS, COX-2 and MMP-9 (Fig. 2-B and 3A-C).

We then used RT-PCR to study the effects of blockade of NOS with L-NAME on MMP-9 and COX-2 mRNA levels. Inhibition of NOS with L-NAME downregulated the expression of COX-2. This is not surprising since NO is known to stimulate the activity of cyclooxygenase (Salvemini et al., 1993) and NO stimulates COX-2 mRNA expression in rat mesangial cells (Tetsuka et al., 1996). Interestingly, we have found that MMP-9 mRNA upregulation was inhibited by L-NAME showing that MMP-9 induction is NO-dependent by a NOS-dependent mechanism. This observation was confirmed and quantified by real time PCR experiments (Fig. 5-A).

Initially it was thought that NO-effects could potentially be mediated through either nitrosylation, oxidation, nitration or a combination of these reactions, since these non-specific reactions are common in inflammatory settings. Peroxynitrite is one of the most reactive biochemical fates of NO and in many studies has been described as a signaling molecule that acts through tyrosine nitration (Patel et al., 1999). For this reason, SOD and membrane-soluble SOD mimetic MnTMPyP were used to investigate ONOO⁻ effects on the MMP-9 induction pathway. The treatments did not modify the MMP-9 gene control mechanism suggesting that ONOO⁻ was not involved in this process (Fig. 6-A and B). A second pathway by which NO could be acting was through soluble guanylate cyclase. Our results indicated that in the presence of ODQ, an inhibitor of soluble guanylate cyclase, the MMP-9 mRNA returned to its basal levels. Furthermore, the effect produced by

13

ODQ was reversed by exogenous 8-bromo-cGMP, a soluble analog of cGMP (Fig. 7-B). These data imply that the soluble guanylate cyclase was the main pathway for NO-dependent MMP-9 gene upregulation.

Recently, in contrast to our results on enhancement of MMP-9 (Eberhardt et al., 2000), using rat mesangial cells found that endogenous or exogenously provided NO decreased MMP-9 gene expression. They also showed that administration of another inhibitor of NOS, L-NMMA increased MMP-9 mRNA expression. NO can reduce t1/2 life of MMP-9 mRNA (Eberhardt et al., 2002) as well as S-nitrosylate NF-kB (Marshall and Stamler, 2001), two mechanisms by which NO may modulate MMP-9 expression. By contrast NO has been found to increase MMP-9 activity through s-nitrosylation (Gu et al., 2002).

Interestingly, pharmacological studies using L-NAME (inhibitor of NOS) and AMD6221 (NO scavenger) yielded contradictory data on MMP-9 activity. The administration of L-NAME to neonatal hyperoxic rats increased activity of MMP-9 (Radomski et al., 1998), while NO scavenging decreased MMP-9 activity elevated by extracorporeal circulation (Mayers et al., 2003). These complex effects of inhibition by NO of expression and activity of MMP-9 likely reflect dual nature of NO as inflammatory-inhibitor and inflammatory-mediator (Droge, 2002).

The conflicting results on enhancement or inhibition of MMP-9 illustrate the complexity of the interactions of NO with cell signalling cascades. Factors such as cell type, stimulation time and stimulatory cocktail likely contribute to some of the differences observed. In our study we examined the expression of MMP-9 mRNA after 12h of treatment using a cocktail containing LPS, IFN-γ and PMA and observed that serum starved cells even in the absence of the stimulatory cocktail (control conditions) began to synthesize MMP-9 mRNA by 24h. These results were further validated by a time course of MMP-9 activity, using zymography, in which 12h was clearly the optimal induction time as described above. It is possible that in settings where cells have been stimulated for 24 to 72h, as done in several of the studies outlined above (Eberhardt et al., 2000; Eberhardt et al., 2002), the levels of NO are different than we have observed. A time course of NO_2^- formation using the Griess reaction showed that there was a significant increase in nitrite formation after 24h and after 48h of cell activation whereas nitrite formation could not be detected in control conditions or when activated cells were co-treated with either L-NAME or 1400W.

Thus, NO may function through alternative pathways to reduce MMP-9 levels, e.g. through oxidation of MMP-9 mRNA. Our findings could be interpreted in terms of early and late NO-mediated events, in which

NO concentration and exposure time are critical in dictating outcomes. Future experiments must attempt to clarify the underling causes of the contradictory results in the literature.

The list of genes that are upregulated via soluble guanylate cyclase-mediated pathways includes only COX-2, TNF, PAI-1, FLT-1, MKP-1 (Pfeilschifter et al., 2001) and now MMP-9. The exact mechanism by which cGMP exerts its transcription regulatory functions has not been fully elucidated. Activated soluble guanylate cyclase synthesizes cGMP, which in turn alters the activity of three main target proteins: (1) cGMP-regulated ion channels, (2) cGMP-regulated phosphodiesterases, and (3) cGMP-dependent protein kinases (PKG). Several lines of evidence appear to involve PKG as the mediator of soluble guanylate cyclase action on MMP-9 gene (Gudi et al., 1996; Gudi et al., 1997; Gudi et al., 1999). More recent studies have shown that PKG-mediated gene regulation takes place via activation of members of the MAPK protein family including Raf1, ERK1/2 and synthesis of c-jun. Interestingly, protein kinase C (PKC) has been shown to regulate transcription of MMP-9 gene via stimulation of ERK1/2 pathway (Genersch et al., 2000; Lee et al., 2003). This PKC-like behavior may partially explain how increased soluble guanylate cyclase activity upregulates MMP-9 gene. However, under conditions of our experiments stimulation of PKG, but not PKC, appears to be necessary for MMP-9 gene induction since despite the continuous presence of PMA, a known stimulator of PKC (Ron and Kazanietz, 1999), the blockade of soluble guanylate cyclase pathway with ODQ abolished MMP-9 gene transcription.

The precise mechanisms involved in soluble guanylate cyclase-mediated MMP-9 gene induction remain to be studied. It is important to note that our current understanding of regulatory mechanisms of the MMP-9 promoter is very limited. Transcription Elements Search System (TESS) analysis of 1300bp of the rat MMP-9 promoter reveals a complex picture of multiple binding sites for more than 200 different transcription factors. We are currently investigating the relevance of a novel PKG/PKA target, which we have identified as a possible MMP-9 repressor.

The results of our experiments show that the NO-cGMP pathway plays a crucial role in MMP-9 gene regulation. The pharmacological significance of our findings remains to be studied.

JPET #050385

16

Reference:

Albert J, Radomski A, Soop A, Sollevi A, Frostell C and Radomski MW (2003) Differential release of matrix metalloproteinase-9 and nitric oxide following infusion of endotoxin to human volunteers. *Acta Anaesthesiol Scand* **47**:407-410.

Alexander C and Rietschel ET (2001) Bacterial lipopolysaccharides and innate immunity. *J Endotoxin Res* **7**:167-202.

Beckman JS, Beckman TW, Chen J, Marshall PA and Freeman BA (1990) Apparent hydroxyl radical production by peroxynitrite: implications for endothelial injury from nitric oxide and superoxide. *Proc Natl Acad Sci U S A* **87**:1620-1624.

Beckman JS and Koppenol WH (1996) Nitric oxide, superoxide, and peroxynitrite: the good, the bad, and ugly. *Am J Physiol* **271**:C1424-1437.

Bone RC (1994) Gram-positive organisms and sepsis. *Arch Intern Med* **154**:26-34.

Droge W (2002) Free radicals in the physiological control of cell function. *Physiol Rev* **82**:47-95.

Dubois B, Starckx S, Pagenstecher A, Oord J, Arnold B and Opdenakker G (2002) Gelatinase B deficiency protects against endotoxin shock. *Eur J Immunol* **32**:2163-2171.

Eberhardt W, Akool el S, Rebhan J, Frank S, Beck KF, Franzen R, Hamada FM and Pfeilschifter J (2002) Inhibition of cytokine-induced matrix metalloproteinase 9 expression by peroxisome proliferator-activated receptor alpha agonists is indirect and due to a NO-mediated reduction of mRNA stability. *J Biol Chem* **277**:33518-33528.

Eberhardt W, Beeg T, Beck KF, Walpen S, Gauer S, Bohles H and Pfeilschifter J (2000) Nitric oxide modulates expression of matrix metalloproteinase-9 in rat mesangial cells. *Kidney Int* **57**:59-69.

Ermert M, Merkle M, Mootz R, Grimminger F, Seeger W and Ermert L (2000) Endotoxin priming of the cyclooxygenase-2-thromboxane axis in isolated rat lungs. *Am J Physiol Lung Cell Mol Physiol* **278**:L1195-1203.

Fischer LG, Hollmann MW, Horstman DJ and Rich GF (2000) Cyclooxygenase inhibitors attenuate bradykinin-induced vasoconstriction in septic isolated rat lungs. *Anesth Analg* **90**:625-631.

Genersch E, Hayess K, Neuenfeld Y and Haller H (2000) Sustained ERK phosphorylation is necessary but not sufficient for MMP-9 regulation in endothelial cells: involvement of Ras-dependent and - independent pathways. *J Cell Sci* **113**:4319-4330.

Gilchrist M, Savoie M, Nohara O, Wills FL, Wallace JL and Befus AD (2002) Nitric oxide synthase and nitric oxide production in in vivo-derived mast cells. *J Leukoc Biol* **71**:618-624.

Gomez-Jimenez J, Salgado A, Mourelle M, Martin MC, Segura RM, Peracaula R and Moncada S (1995) L-arginine: nitric oxide pathway in endotoxemia and human septic shock. *Crit Care Med* **23**:253-258.

Grisham MB, Jourd'Heuil D and Wink DA (1999) Nitric oxide. I. Physiological chemistry of nitric oxide and its metabolites:implications in inflammation. *Am J Physiol* **276**:G315-321.

Gu Z, Kaul M, Yan B, Kridel SJ, Cui J, Strongin A, Smith JW, Liddington RC and Lipton SA (2002) S-nitrosylation of matrix metalloproteinases: signaling pathway to neuronal cell death. *Science* **297**:1186-1190.

Gudi T, Hong GK, Vaandrager AB, Lohmann SM and Pilz RB (1999) Nitric oxide and cGMP regulate gene expression in neuronal and glial cells by activating type II cGMP-dependent protein kinase. *Faseb J* **13**:2143-2152.

Gudi T, Huvar I, Meinecke M, Lohmann SM, Boss GR and Pilz RB (1996) Regulation of gene expression by cGMP-dependent protein kinase. Transactivation of the c-fos promoter. *J Biol Chem* **271**:4597-4600.

Gudi T, Lohmann SM and Pilz RB (1997) Regulation of gene expression by cyclic GMP-dependent protein kinase requires nuclear translocation of the kinase: identification of a nuclear localization signal. *Mol Cell Biol* **17**:5244-5254.

Knuefermann P, Nemoto S, Baumgarten G, Misra A, Sivasubramanian N, Carabello BA and Vallejo JG (2002) Cardiac inflammation and innate immunity in septic shock: is there a role for toll-like receptors? *Chest* **121**:1329-1336.

Lee WJ, Shin CY, Yoo BK, Ryu JR, Choi EY, Cheong JH, Ryu JH and Ko KH (2003) Induction of matrix metalloproteinase-9 (MMP-9) in lipopolysaccharide-stimulated primary astrocytes is mediated by extracellular signal-regulated protein kinase 1/2 (Erk1/2). *Glia* **41**:15-24.

Marshall HE and Stamler JS (2001) Inhibition of NF-kappa B by S-nitrosylation. *Biochemistry* **40**:1688-1693.

JPET #050385

Mayers I, Hurst T, Radomski A, Johnson D, Fricker S, Bridger G, Cameron B, Darkes M and Radomski MW (2003) Increased matrix metalloproteinase activity after canine cardiopulmonary bypass is suppressed by a nitric oxide scavenger. *J Thorac Cardiovasc Surg* **125**:661-668.

Ohara Y, Peterson TE and Harrison DG (1993) Hypercholesterolemia increases endothelial superoxide anion production. *J Clin Invest* **91**:2546-2551.

Opdenakker G (2001) New insights in the regulation of leukocytosis and the role played by leukocytes in septic shock. *Verh K Acad Geneeskd Belg* **63**:531-538; discussion 538-541.

Patel RP, McAndrew J, Sellak H, White CR, Jo H, Freeman BA and Darley-Usmar VM (1999) Biological aspects of reactive nitrogen species. *Biochim Biophys Acta* **1411**:385-400.

Pfeilschifter J, Eberhardt W and Beck KF (2001) Regulation of gene expression by nitric oxide. *Pflugers Arch* **442**:479-486.

Pugin J, Widmer MC, Kossodo S, Liang CM, Preas HLn and Suffredini AF (1999) Human neutrophils secrete gelatinase B in vitro and in vivo in response to endotoxin and proinflammatory mediators. *Am J Respir Cell Mol Biol* **20**:458-464.

Radomski A, Sawicki G, Olson DM and Radomski MW (1998) The role of nitric oxide and metalloproteinases in the pathogenesis of hyperoxia-induced lung injury in newborn rats. *Br J Pharmacol* **125**:1455-1462.

Radomski MW, Vallance P, Whitley G, Foxwell N and Moncada S (1993) Platelet adhesion to human vascular endothelium is modulated by constitutive and cytokine induced nitric oxide. *Cardiovasc Res* **27**:1380-1382.

Ritzel MW, Ng AM, Yao SY, Graham K, Loewen SK, Smith KM, Ritzel RG, Mowles DA, Carpenter P, Chen XZ, Karpinski E, Hyde RJ, Baldwin SA, Cass CE and Young JD (2001) Molecular identification and characterization of novel human and mouse concentrative Na+-nucleoside cotransporter proteins (hCNT3 and mCNT3) broadly selective for purine and pyrimidine nucleosides (system cib). *J Biol Chem* **276**:2914-2927.

Ron D and Kazanietz MG (1999) New insights into the regulation of protein kinase C and novel phorbol ester receptors. *Faseb J* **13**:1658-1676.

Salvemini D, Misko TP, Masferrer JL, Seibert K, Currie MG and Needleman P (1993) Nitric oxide activates cyclooxygenase enzymes. *Proc Natl Acad Sci U S A* **90**:7240-7244.

Strong VE, Mackrell PJ, Concannon EM, Naama HA, Schaefer PA, Shaftan GW, Stapleton PP and Daly JM (2000) Blocking prostaglandin E2 after trauma attenuates pro-inflammatory cytokines and improves survival. *Shock* **14**:374-379.

Szabo C, Zingarelli B and Salzman AL (1996) Role of poly-ADP ribosyltransferase activation in the vascular contractile and energetic failure elicited by exogenous and endogenous nitric oxide and peroxynitrite. *Circ Res* **78**:1051-1063.

Szkotak AJ, Ng AM, Sawicka J, Baldwin SA, Man SF, Cass CE, Young JD and Duszyk M (2001) Regulation of K(+) current in human airway epithelial cells by exogenous and autocrine adenosine. *Am J Physiol Cell Physiol* **281**:C1991-2002.

Tetsuka T, Daphna-Iken D, Miller BW, Guan Z, Baier LD and Morrison AR (1996) Nitric oxide amplifies interleukin 1-induced cyclooxygenase-2 expression in rat mesangial cells. *J Clin Invest* **97**:2051-2056.

Titheradge MA (1999) Nitric oxide in septic shock. *Biochim Biophys Acta* **1411**:437-455.

Webber D (1998) Restored credibility for sepsis therapeutics? *Nat Biotechnol* **16**:1303.

JPET #050385

Oncology, University of Alberta, Edmonton, Alberta, Canada (2); Department of Integrative Biology and

Pharmacology, University of Texas, Health Sciences Center at Houston (3); the Cross Cancer Institute (4) and

Pulmonary Research Group (5), Edmonton, Alberta, Canada.

Address correspondence to: Dr. A. Dean Befus, AstraZeneca Canada Inc., Chair in Asthma Research,

Glaxo-Heritage Asthma Research Laboratories, Department of Medicine, University of Alberta, Edmonton,

AB, T6G 2S2, Canada. E-mail: dean.befus@ualberta.ca

Legends for figures:

Fig. 1: Fluorescence detection of intracellular NO production. Cells were either serum starved (A and B) or treated with a cocktail containing PMA, LPS and IFNγ (C and D), for 12h then stained with DAF for 1h. DAF fluorescence (white in the figure) was analyzed with confocal analysis. Differential interference contrast combined with DAF (B and D) shows cellular morphology (bars = 50μm).

Fig. 2: Characterization of the septic shock model at the transcriptional level. (A) A7r5 cells were treated with a cocktail of pro-inflammatory substances (refer to materials and methods) to induce the production of iNOS, COX-2 and MMP-9. The 100bp DNA ladder marker provides an estimate of the size of each PCR product ($n = 6$). (B) RT-PCR was used to investigate the mRNA levels corresponding to each gene. Cells were, untreated (Sham), induced with the activating cocktail (Activated), or incubated with Dexamethasone (Dex) 1 h before activation. GAPDH was used as the positive control for each experiment ($n = 3$). (C) Densitometric analysis for RT-PCR experiments shown in (B) ($n = 3$). Statistical significance: P<0.001 (***), (†††).

Fig. 3: Characterization of the septic shock model at the protein level. To further investigate the expression of MMP-9, iNOS, and COX-2, we estimated protein expression levels using immuno-blot. A7r5 cells were untreated (Sham), activated with a cocktail (Activated) or pre-incubated with dexamethasone 1 h prior to activation. (A) The pro and active form of MMP-9 at 92 and 88 kDa were detected. Active MMP-9 was significantly upregulated in the activated cells. Pretreatment with Dexamethasone significantly reduced MMP-9 induction ($n = 3$). (B) The inducible form of NOS (iNOS) appeared as a band at 130 kDa. Significant differences were found between the sham and activated groups. Also significant differences were obtained when iNOS induction was inhibited with dexamethasone ($n = 3$). (C) Similar results to those in panel A and B were obtained for the COX-2 protein at 74 kDa. A second band at a higher molecular weight also appeared only in activated conditions and was suspected to be due to antibody cross-reactivity ($n = 3$). Statistical significance: P<0.01 (**), (††); P<0.001 (***), (†††).

Fig. 4: MMP-9, iNOS and COX-2 enzymatic activity in A7r5 cells. A7r5 cells were untreated (Sham), activated with a cocktail (Activated) or pre-incubated with dexamethasone 1 h prior to activation. (A) Inducible NOS activity was measured using the citrulline assay. Significant changes between sham and activated conditions were found (p = 0.027), but for iNOS there were no significant changes between sham and dexamethasone treatment (Dex). The cNOS activity, also measured with this assay, was not detected after

each treatment ($n = 3$). (B) PGE$_2$ formation was monitored using ELISA. Significant changes were observed between sham and activated cells, as well as between activated and Dexamethasone treatment ($n = 4$). (C) Zymography was performed to measure the gelatinolytic activity of MMP-9. The pro and active forms of MMP-9 were detected at 92 and 88 kDa respectively. At 72 and 62 kDa the pro and active forms of MMP-2 were also detected. MMP-2 is a constitutive metalloproteinase that remained relatively unchanged despite different treatments. Densitometric analysis for MMP-9 and MMP-2 revealed a highly significant upregulation in activity of MMP-9 in activated cells, whereas dexamethasone (Dex) inhibited this upregulation to near control levels ($n = 3$). Statistical significance: $P<0.05$ (*), (†); $P<0.01$ (**), (††); $P<0.001$ (***), (†††).

Fig. 5: Effect of L-NAME treatment on levels of mRNA for iNOS, COX-2 and MMP-9. (A) RT-PCR was performed using both Dexamethasone (Dex) and L-NAME as pharmacological tools. The positive control GAPDH was constant for each treatment. L-NAME had an inhibitory effect obvious for COX-2 and for MMP-9 ($n = 3$). (B) Real time PCR was performed to validate and quantify the RT-PCR findings. MMP-9 mRNA upregulation was found to be of 11.7 fold. This effect was inhibited by both, Dexamethasone and L-NAME to levels relatively close to sham ($n = 3$). (C) COX-2 upregulation during activation was found to be 2.3 fold and this effect was inhibited to lower than sham levels when treating with either Dexamethasone or L-NAME ($n = 3$). Statistical significance: $P<0.05$ (*), (†); $P<0.01$ (**), (††).

Fig. 6: MMP-9 gene induction is not mediated by ONOO$^-$. (A) An SOD concentration dependence curve was created. Cells were left untreated (Sham) or induced with the activating cocktail containing different concentrations of SOD. No significant variations were observed when comparing maximum activation (0.0 U/mL SOD) with activation in the presence of SOD (100 to 0.5 U/mL SOD) ($n = 3$). (B) The SOD mimetic MnTMPyP (0-20µM) did not exert a significant reduction of MMP-9 mRNA relative abundance ($n = 3$). Statistical significance: $P<0.05$ (*).

Fig. 7: Nitric Oxide upregulates MMP-9 via a soluble guanylate cyclase-dependent pathway. Relative abundance of MMP-9 mRNA was measured using real time PCR. (A) There was a significant upregulation of the MMP-9 gene when inducing A7r5 cells with the activating cocktail (Activated). When cells were activated in the presence of ODQ (0.05 to 5 µM), this resulted in a significant decrease in the MMP-9 mRNA levels. It was shown that at a concentration of 0.5µM ODQ, the activating cocktail did not induce any

JPET #050385

significant changes in the MMP-9 mRNA levels ($n = 3$). (B) Exogenously added 8-bromo-cGMP (0 to

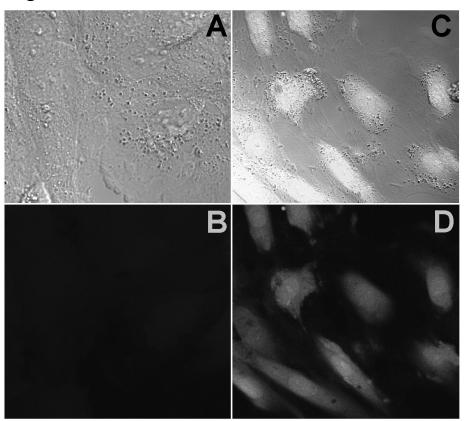0.5mM) reversed the effect of ODQ (0.5μM). Statistical significance: P<0.05 (*), (†).

Table 1: Summary of RT-PCR primer details.

MRNA	Primer Position (5' to 3')	PCR product size (bp)	Primer sequence (5' to 3')	Annealing temperature (^{o}C)	Accession number
F-MMP-9	141-164	241	gga tta cct gta ccg cta tgg tta	55	NM_031055
R-MMP-9	381-358		ttg gat cca ata ggt gat gtt atg		
F-COX-2	331-354	664	cac ccc aaa cac agt aca cta cat	58	S67722
R-COX-2	994-971		gat ggt agc ata cat cat cag acc		
F-iNOS	227-250	347	caa gct gta tgt gac tcc atc gac	55	D14051
R-iNOS	573-549		aga tga gct cat cca gag tga gct g		
F-GAPDH	331-350	528	acc acc atg gag aag gct gg	55	NM_017008
R-GAPDH	858-839		ctc agt gta gcc cag gat gc		

Table 2: Summary of Real time PCR primer and probe sequences and accession numbers.

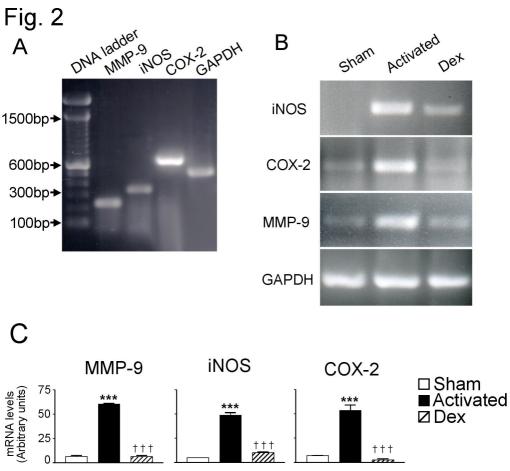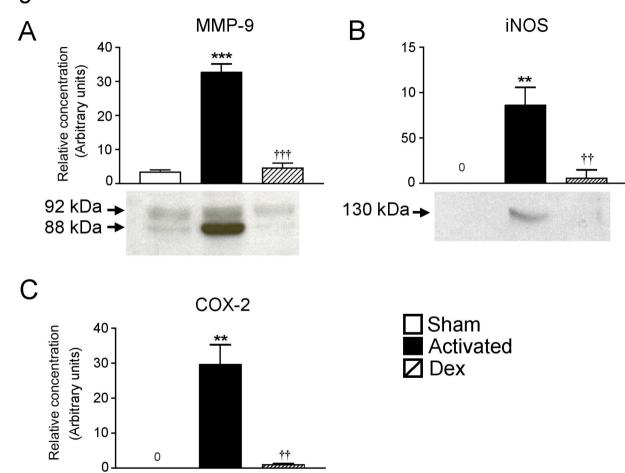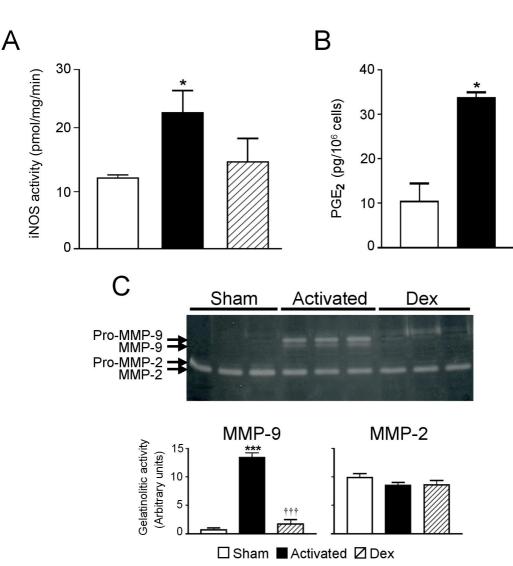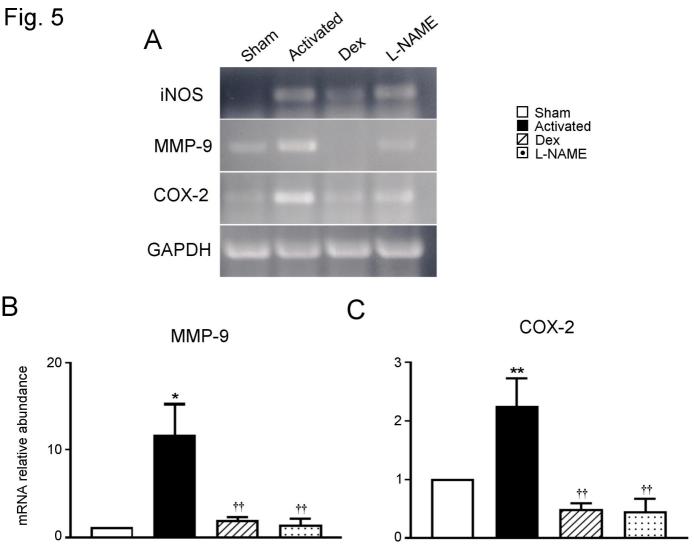| MRNA	Primer sequence (5' to 3')	Probe sequence (5' to 3')	Accession number
F-MMP-9	cag acc aag ggt aca gcc tgt t	6FAM-5'-ctg gtg gca gcg ca	NM_031055
R-MMP-9	agc gca tgg ccg aac tc		
F-COX-2	tcc agc tca cgg tac cag aag	6FAM-5'-tag gcc cca tgc aat	S67722
R-COX-2	gca tcc agg ctg aac tca ca		
F-iNOS	gga ttt tcc cag gca acc a	6FAM-5'-acg gcc ctg gtg ca	D14051
R-iNOS	tcc aca act cgc tcc aag atc		
F-GAPDH	cct gga gaa acc tgc caa gta t	6FAM-5'-atg aca tca aga agg tgg	NM_017008
R-GAPDH	ctc ggc cgc ctg ctt		

Fig. 1

Fig. 2

A

B

C

MMP-9   iNOS   COX-2

mRNA levels (Arbitrary units)

75

50

25

□ Sham
■ Activated
▨ Dex

***   †††

Fig. 3

A

MMP-9

92 kDa →
88 kDa →

B

iNOS

130 kDa →

C

COX-2

74 kDa →

☐ Sham
■ Activated
▨ Dex

Fig. 4

Fig. 5

Fig. 6

Fig. 7